p53 is associated with cellular microtubules and is transported to the nucleus by dynein

Paraskevi Giannakakou*†, Dan L. Sackett‡, Yvona Ward*, Kevin R. Webster§, Mikhail V. Blagosklonny* and Tito Fojo*

*Medicine Branch, Division of Clinical Sciences, National Cancer Institute, National Institutes of Health, 9000 Rockville Pike, Bethesda, Maryland 20892, USA
‡Laboratory of Integrative and Medical Biophysics, National Institute of Child Health and Human Development, National Institutes of Health, 9000 Rockville Pike, Bethesda, Maryland 20892, USA
§Bristol–Myers Squibb Pharmaceutical Research Institute, Department of Oncology Drug Discovery, PO Box 4000, Princeton, New Jersey. 08543-4000, USA
†e-mail: evigi@box-e.nih.gov

Here we show that p53 protein is physically associated with tubulin *in vivo* and *in vitro*, and that it localizes to cellular microtubules. Treatment with vincristine or paclitaxel before DNA-damage or before leptomycin B treatment reduces nuclear accumulation of p53 and expression of mdm2 and p21. Overexpression of dynamitin or microinjection of anti-dynein antibody before DNA damage abrogates nuclear accumulation of p53. Our results indicate that transport of p53 along microtubules is dynein-dependent. The first 25 amino acids of p53 contain the residues that are essential for binding to microtubules. We propose that functional microtubules and the dynein motor protein participate in transport of p53 and facilitate its accumulation in the nucleus after DNA damage.

The tumour-suppressor protein p53 is involved in cell-cycle control, apoptosis, differentiation, DNA repair and recombination, and centrosome duplication[1–5]. In response to DNA damage, p53 accumulates in the nucleus[6–8], where it transcriptionally activates the genes that encode $p21^{CIP1/WAF1}$ and mdm2, as well as other genes that are involved in growth arrest and apoptosis[1,2,9–11].

Inactivation of p53 is the most common alteration found in human cancer[12,13]. Although acquired mutations that affect its transactivating function are the most frequent and the best known, there are other mechanisms by which p53 can be inactivated[1,14–16]. One poorly understood mechanism of p53 inactivation involves its exclusion from the nucleus[17–19]; cytoplasmic accumulation of p53 is an independent prognostic indicator in cancer[20,21]. In some cells, p53 is sequestered in the cytoplasm and seems less responsive to DNA damage[17]. Although the mechanisms that regulate the subcellular localization of p53 in cells are unknown, they may involve tethering to cytoplasmic or nuclear structures[22].

Here we investigate a potential interaction between p53 and the tubulin/microtubule cytoskeleton. We show that p53 is associated with tubulin both *in vivo* and *in vitro*, that it associates preferentially with the polymerized form of tubulin (microtubules), and that this interaction is lost after treatment with microtubule-depolymerizing drugs. Using four human cancer cell lines of distinct origins, we demonstrate, by confocal microscopy, that p53 associates with cellular microtubules and accumulates in the nucleus after DNA damage only in cells with a functional microtubule network. Disruption of normal microtubule dynamics, whether by stabilization with paclitaxel or depolymerization with vincristine, compromises microtubule function. Both of these drug treatments impair nuclear accumulation of p53 after DNA damage. In addition, overexpression of dynamitin, which is known to dissociate the microtubule-associated motor protein dynein from microtubules, results in impaired accumulation of p53 in the nucleus following DNA damage, indicating that dynein may be necessary for transport of p53 on microtubules. Similar results were obtained after microinjection of an antibody against the dynein intermediate chain (70.1), further supporting the idea that dynein functions in p53 transport. Finally, we report that the microtubule-binding domain of p53 is contained within its first 25 amino acids. These findings document an important mechanism that regulates the subcellular localization of p53 and its downstream signalling.

Results

Wild-type and mutant p53 co-precipitate with α/β-tubulin *in vivo*. To determine whether p53 associates with tubulin *in vivo*, we carried out co-immunoprecipitation experiments (Fig. 1). We incubated whole-cell lysates from A2780 (1A9) human ovarian carcinoma cells with anti-tubulin antibodies, for immunoprecipitation followed by immunoblotting with an anti-p53 antibody (Fig. 1a). Because tubulin is a dimer composed of α/β-tubulin subunits, immunoprecipitations were carried out using either anti-α- or anti-β-tubulin antibodies. As shown in Fig. 1a, p53 protein was present in immunoprecipitates obtained with either anti-α-, anti-β- or both anti-tubulin antibodies. To investigate whether this p53–tubulin association occurs only with wild-type p53, we carried out the same experiment using 1A9/PTX22 cells, a paclitaxel-resistant subline[23], with high levels of mutant p53 (ref. 24). As was found for the wild-type protein, mutant p53 co-precipitated with either anti-α-, anti-β- or both anti-tubulin antibodies. That p53 associates with tubulin was further confirmed by the fact that two different anti-p53 antibodies co-precipitated tubulin (Fig. 1b).

To exclude the possibility that anti-p53 antibodies bind to tubulin in a non-specific manner, we carried out co-immunoprecipitation assays using purified rat-brain microtubule (RBMT) protein or lysates from p53-null PC3 human prostate carcinoma cells (Fig. 1c). Neither anti-p53 antibody precipitated RBMT protein, nor did they precipitate tubulin from PC3 cells. Furthermore, to exclude non-specific 'cytoplasmic trapping' of p53, we investigated the association of p53 with another cytoplasmic protein, vimentin. Figure 1d shows that the anti-p53 antibody did not co-precipitate vimentin from lysates of 1A9 or 1A9/PTX22 cells.

Co-polymerization of wild-type and mutant p53 with microtubules. We next investigated whether p53 binds to soluble tubulin dimers, polymerized tubulin (microtubules), or both. We carried

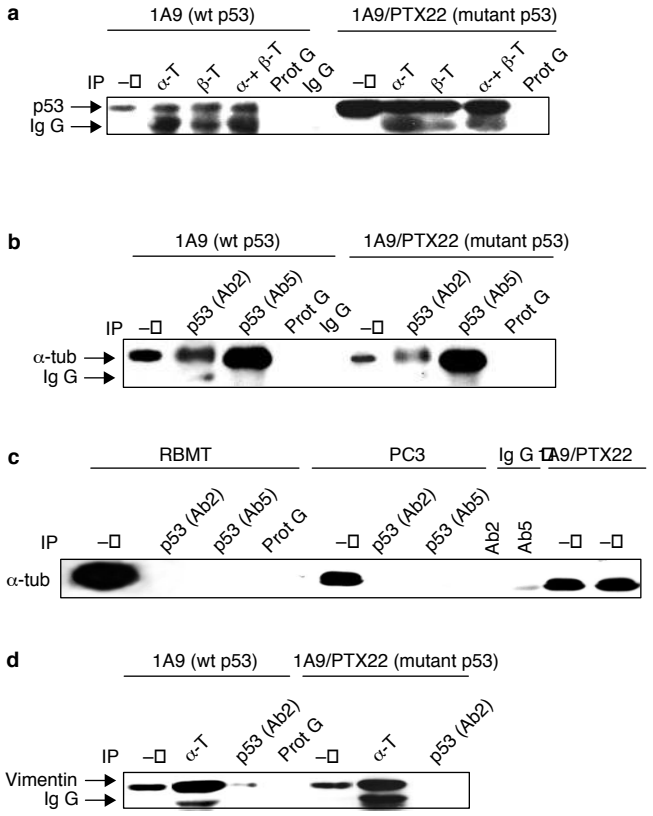

Figure 1 **p53 co-immunoprecipitates with tubulin. a–c**, Co-immunoprecipitation (IP) experiments, using the human ovarian carcinoma cell line 1A9, with wild-type p53, and its paclitaxel-resistant subline 1A9/PTX22, with mutant p53 protein. **a**, 1 mg of soluble cell protein from each cell line was immunoprecipitated with anti-α-tubulin (α-T), anti-β-tubulin (β-T) or both anti-tubulin antibodies, as indicated, and immunoblotted with an anti-p53 antibody (Ab2). Lanes marked with a minus sign were loaded with 50 μg of soluble cell protein which had not been subjected to immunoprecipitation. Prot G, 1 mg of soluble cell protein immunoprecipitated only with protein G–agarose beads, in the absence of the antibody, as a negative control; Ig G, antibody used for IP, loaded alone. **b**, 1 mg of soluble cell protein from each cell line was immunoprecipitated with anti-p53 antibodies (Ab2 or Ab5) as indicated, and immunoblotted with an anti-α-tubulin antibody. Lanes marked with a minus sign, Prot G and Ig G were loaded as in **a**. **c**, Anti-p53 antibodies do not crossreact with tubulin. 1 mg ml^{-1} of purified rat-brain microtubule (RBMT) protein or 1 mg of soluble cell protein from PC3 cells (p53-null) were immunoprecipitated with anti-p53 antibodies (Ab2 or Ab5) as indicated, and probed for β-tubulin. Purified RBMT protein (5 μg) or soluble cell protein (50 μg) from PC3, 1A9 or 1A9/PTX22 cells were loaded as controls. Prot G, negative control, involving immunoprecipitation only with protein G–agarose in the absence of antibody. Lanes labelled Ab2 and Ab5 were loaded only with the anti-p53 antibodies used for IP. **d**, 1 mg of soluble cell protein from 1A9 or 1A9/PTX22 cells was immunoprecipitated with anti-α-tubulin or anti-p53 (Ab2) antibodies as indicated, and immunoblotted with an anti-vimentin antibody. Lanes marked with a minus sign were loaded with 50 μg of soluble cell protein which had not been subjected to immunoprecipitation. Prot G, negative control, containing 1 mg of soluble cell protein immunoprecipitated only with protein G–agarose beads, in the absence of the antibody.

out successive cycles of temperature-dependent polymerization and depolymerization of tubulin (Fig. 2a) by adding purified RBMT protein to extracts of 1A9 cells (wild-type p53; Fig. 2b, upper panel) and 1A9/PTX22 cells (mutant p53; Fig. 2b, middle panel). We separated comparable amounts of protein from each fraction by SDS–polyacrylamide-gel electrophoresis (SDS–PAGE) and immunoblotted the samples with anti-p53 and anti-tubulin antibodies. Both wild-type and mutant p53 co-fractionated with the microtubule pellets after the polymerization cycle (warm pellet, WP). In addition, p53 remained associated with 'cold-stable' microtubules in the cold pellet (CP) fraction after the depolymerization cycle. RBMT protein loaded as a control was not associated with any p53, excluding the possibility of non-specific background staining. Tubulin, as soluble dimers (Fig. 2b; HSS, high-speed supernatant; WS, warm supernatant; CS, cold supernatant) or microtubules (Fig. 2b; HSP, WP, CP) was detected in every fraction. To rule out non-specific 'trapping' of p53 in microtubule pellets, we reprobed the same blot for mdm2 and p21. Both mdm2 and p21 segregated with warm supernatant fraction, unlike p53 which segregated with the microtubule pellet (WP). Neither mdm2 nor p21 was detected in the subsequent fractions (CP, CS), as only the WP fraction was used for this cycle. Figure 2c shows the results of treatment of cells expressing wild-type (1A9) or mutant (1A9/PTX22) p53 with the microtubule-depolymerizing agent colchicine, followed by immunoprecipitation with the anti-p53 antibody Ab7 and immunoblotting with an anti-α-tubulin antibody. Treatment with colchicine resulted in a marked reduction in the amount of tubulin co-precipitated with p53, indicating that depolymerization of microtubules causes p53 to dissociate from microtubules, and further supporting the idea that p53 preferentially associates with microtubules rather than tubulin subunits.

p53 co-localizes with cellular microtubules *in vivo*. Using immunofluorescent staining of p53 (Texas Red) and α-tubulin (fluorescein isothiocyanate, FITC) we investigated the subcellular localization of p53 and its association with microtubules *in vivo*. We determined the localization by confocal microscopy in 1A9 human ovarian carcinoma (wild-type p53), A498 human renal carcinoma (wild-type p53), A549 human lung carcinoma (wild-type p53) and PC3 human prostate carcinoma (p53-null) cells (Fig. 3a). In untreated 1A9, A498 and A549 cells (Fig. 3a, left panels), p53 co-localized with the cytoplasmic microtubule network, as shown by the similar patterns of anti-p53 (red) and anti-tubulin (green) staining and confirmed by the yellow colour that is apparent in the overlays. Treatment with the DNA-damaging agent adriamycin (ADR), increased p53 levels and nuclear p53 accumulation in all cells expressing wild-type p53 (Fig. 3a, right panels). In interphase nuclei, which are devoid of microtubules, only red p53 staining was observed, whereas the remaining cytoplasmic p53 was still associated with microtubules. Similar p53/microtubule co-localization was observed in 1A9/PTX22 cells (which express mutant p53; data not shown). Immunostaining of p53 was not detected in PC3 cells (p53-null), which we used as a negative control (Fig. 3a, lower-left panel). We used A549 cells for all subsequent immunofluorescence experiments, because the visualization of their microtubule network was optimal because of their higher cytoplasm/nucleus ratio, larger size and flat shape. Co-immunoprecipitation experiments with p53 and tubulin in these cells confirmed the p53–tubulin association (data not shown). In Fig. 3b, the co-localization of p53 with microtubules is displayed in progressive optical sections along the z-axis in ADR-treated A549 cells. The first optical sections in the sequence, which are focused at the cytoplasm, predominantly show microtubules, whereas the last sections, which are focused above the nucleus, predominantly show p53.

Microtubule-perturbing drugs inhibit nuclear accumulation of p53 after DNA damage. Microtubules are intrinsically dynamic, polarized filaments that are essential for many cellular functions[25], and drugs that affect their dynamic behaviour, including paclitaxel and vincristine, have been used as tools to study microtubule-dependent cellular events[26,27]. We used drugs that either destabilize (vincristine) or stabilize (paclitaxel) microtubules to study the association of p53 with microtubules, the accumulation of p53 in the nucleus after DNA damage, and the ability of p53 to transactivate its target genes (Fig. 4). Treatment of A549 cells with ADR resulted in increased levels of p53, which was predominantly accumulated in

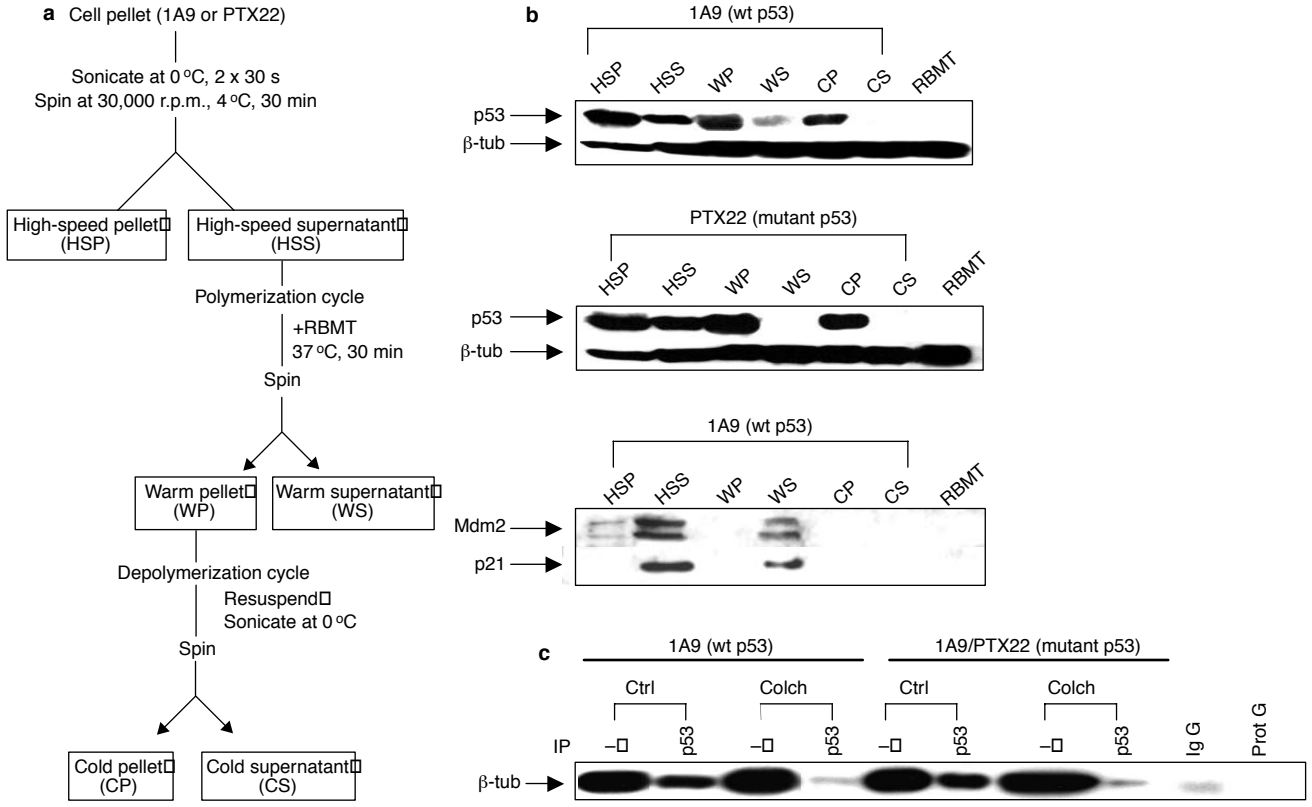

Figure 2 **Wild-type and mutant p53 bind preferentially to polymerized tubulin. a**, Schematic representation of the protocol used for temperature-dependent polymerization and depolymerization of microtubules (see Methods). RBMT, rat-brain microtubule protein. **b**, Proteins from each of the fractions in **a** were immunoblotted with anti-p53 (Ab2) and anti-β-tubulin antibodies. Both wild-type (upper panel) and mutant p53 (middle panel) co-fractionated with the microtubule pellets (WP and CP). Tubulin was detected in every fraction, as soluble dimers (HSS, WS and CS) or as microtubules (HSP, WP and CP). Exogenous RBMT was loaded as a negative control. Lower panel, the same blot as in the upper panel, reprobed for mdm2 and p21. Both mdm2 and p21 co-fractionated with the soluble tubulin (HSS and WS), in contrast to p53, which co-fractionated with the microtubule pellets. The 1A9 cells (upper and lower panels), expressing wild-type p53, were treated with 400 ng ml^{-1} adriamycin for 16 h. **c**, Depolymerization of microtubules abrogates the p53–tubulin association. The 1A9 (wild-type p53) and 1A9/PTX22 (mutant p53) cells were treated with 100 ng ml^{-1} colchicine for 16 h before immunoprecipitation with anti-p53 (Ab7) antibody. Lanes marked with a minus sign were loaded with 50 μg of soluble cell protein which had not been subjected to immunoprecipitation (IP); lanes labelled p53 were loaded with 1 mg of soluble cell protein after immunoprecipiation from either untreated (Ctrl) or colchicine-treated (Colch). Protein blots were immunoblotted with anti-α-tubulin antibody. Prot G, negative control, containing 1 mg of soluble cell protein incubated with protein G–agarose only; Ig G, negative control, involving anti-p53 antibody (Ab7) loaded alone.

the nucleus. However, when we treated A549 cells with vincristine or paclitaxel before treament with ADR (Fig. 4a, VCR/ADR and TX/ADR, respectively), nuclear accumulation of p53 was reduced relative to that observed in cells treated with ADR alone (Fig. 4a). With vincristine treatment, microtubules became depolymerized, as shown by the diffuse cytoplasmic tubulin staining (green) and the loss of the well organized microtubule network seen in untreated cells. A similar diffuse cytoplasmic pattern was seen for p53 immunostaining (red) as a consequence of dissociation from microtubules, together with a marked reduction in nuclear staining. In addition, p53 did not co-localize with soluble α/β dimers, as shown by the absence of yellow colouration in the overlay. Treatment with paclitaxel stabilized microtubules, resulting in distinct microtubule bundles. p53 preferentially associated with these MT-bundles, as shown by the 'bundle' shape of the red p53 immunostaining pattern and the intense yellow bundles in the overlay (Fig. 4a). As was the case with vincristine treatment, pretreatment with paclitaxel reduced the nuclear accumulation of p53. These observations indicate that nuclear translocation of p53 requires a functional microtubule network, disruption of which results in reduced nuclear accumulation.

As a consequence of the impaired nuclear accumulation of p53, impaired induction of p53 target genes was observed (Fig. 4b). Treatment with paclitaxel or vincristine before application of ADR resulted in reduced levels of mdm2 and p21 levels relative to those observed with ADR alone. These results support and extend the confocal analysis showing inhibition of nuclear accumulation of p53 when treatment with microtubule-affecting drugs precedes DNA damage.

Inhibition of nuclear export does not affect nuclear accumulation of p53 after treatment with microtubule-disrupting drugs. It has been reported that the cytoplasmic localization of p53 in some cells is a result of hyperactive nuclear export[28]. To rule out the possibility that the observed reduction in accumulation of p53 in the nucleus after treatment with microtubule-disrupting drugs was a result of increased nuclear export of p53, rather than of inhibition of nuclear import, we carried out immunoblotting and confocal-microscopic analyses (Fig. 5). We added the nuclear-export inhibitor leptomycin B (LPM)[22] either to untreated A549 cells or to cells pretreated with paclitaxel or vincristine, and then processed these cells for immunoblotting for p53 and mdm2 (Fig. 5a) or for confocal microscopy (Fig. 5b). Treatment with LPM alone resulted in increased levels of both p53 and mdm2, as was the case for treatment with ADR alone. In contrast, treatment with LPM or ADR had no effect on expression of mdm2 after disruption of the microtubule

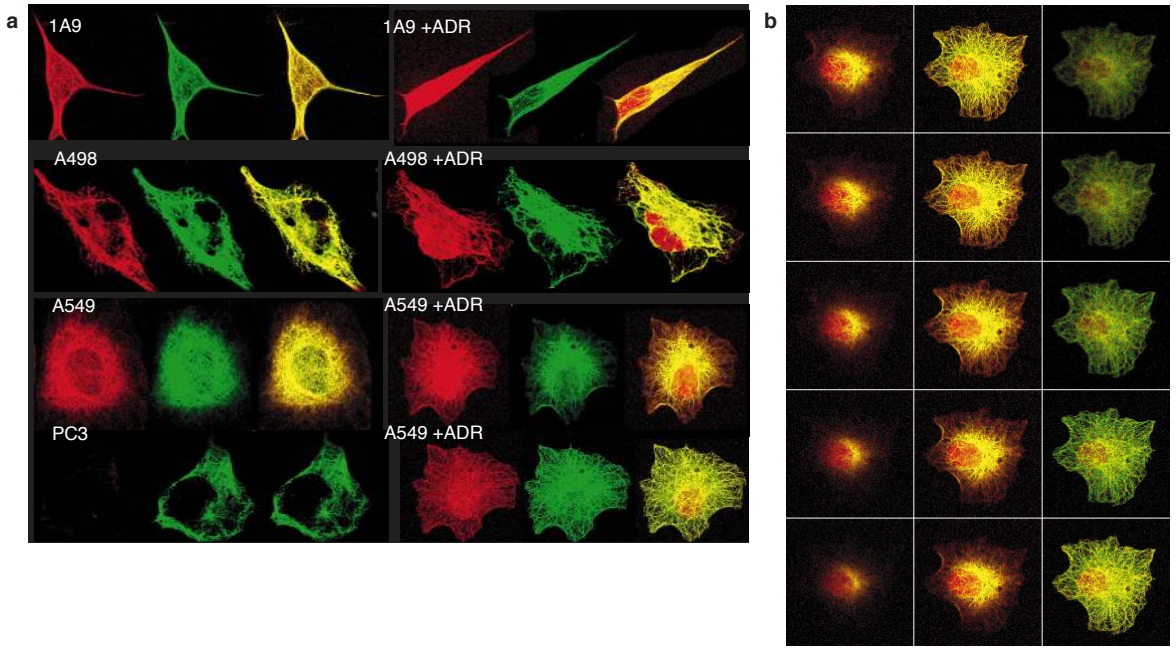

Figure 3 **Co-localization of p53 with cellular microtubules. a**, p53 co-localizes with cellular microtubules. Untreated or adriamycin (ADR)-treated 1A9 human ovarian cancer, A498 human renal cancer and A549 human lung cancer cells were processed for double immunofluorescence labelling with antibodies against p53 (red, labelled with Texas Red) or α-tubulin (green, labelled with FITC). Staining was analysed by confocal laser-scanning microscopy. Co-localization of p53 and tubulin is visible as yellow staining generated where the color images merge. In untreated cells, the p53 staining alone is predominantly cytoplasmic and has a pattern similar to that of tubulin staining alone. Treatment with 400 ng ml^{-1} ADR for 4 h resulted in increased p53 levels and nuclear accumulation of p53 in 1A9, A498 and A549 cells expressing wild-type p53. In overlay images of ADR-treated 1A9, A498, and A549 cells (right), only red p53 staining can be seen in the nucleus, where microtubules are absent, whereas in the cytoplasm, where p53 co-localizes with microtubules, yellow is predominantly seen. For ADR-treated A549 cells (lower-right), two confocal optical sections are shown to emphasize both the accumulation of p53 in the nucleus and the fine reticular microtubule network of p53 in the cytoplasm. Immunostaining of p53 is absent in p53-null PC3 human prostate cancer cells (lower-left), which were used as a negative control. These images represent 3D projections of consecutive optical sections along the z-axis, obtained by confocal microscopy. The only exceptions are the two images showing A549 + ADR, which are individual optical sections focused on two different levels. **b**, Consecutive optical sections along the z-axis of A549 cells treated with ADR. A549 cells were treated with 400 ng ml^{-1} ADR for 4 h and processed for double immunofluorescence labelling with antibodies against p53 (red, labelled with Texas Red) or α-tubulin (green, labelled with FITC). Staining was analysed by confocal laser-scanning microscopy. Images are optical sections at intervals of 0.3 μm along the z-axis from the bottom of the cell to the top of the nucleus.

cytoskeleton with paclitaxel or vincristine, which is consistent with a lack of nuclear accumulation (Fig. 5a). Treatment with LPM alone resulted in accumulation of p53 in the nucleus, compared to a cytoplasmic distribution in untreated cells (Fig. 5b). This accumulation was abrogated by pretreatment with paclitaxel, indicating that p53 cannot translocate to the nucleus and cannot be trapped by LPM. A similar result was obtained with vincristine treatment before treatment with LPM (data not shown), indicating that functional microtubules are required for translocation of p53.

The microtubule-motor complex dynein/dynactin is involved in p53 transport. In most cells, microtubules are organized with their minus ends located near the nucleus and their plus ends towards the cell periphery[27]. Microtubule-based intracellular transport is mediated through the kinesins, which are plus-end-directed microtubule motors, and the dyneins, which are minus-end-directed[29–31]. Both families of microtubule-motor proteins require ATP to move along microtubules with their cargoes.

To investigate whether transport of p53 on microtubules is mediated by motor proteins, we carried out a microtubule co-sedimentation experiment (Fig. 6). We supplemented extracts from ADR-treated A549 cells with exogenous microtubule protein in the presence or absence of AMP-PNP (non-hydrolysable ATP) to induce binding of motors to microtubules (Fig. 6a). After one cycle of polymerization, we separated microtubule proteins by SDS–PAGE and immunoblotted them with anti-p53 antibody. Increased amounts of p53 protein were present in the pellet from the sample that received AMP-PNP relative to that without AMP-PNP, indicating that p53 may be transported along microtubules by a motor protein. We reprobed the same blot either with an antibody against the intermediate chain of cytoplasmic dynein or with antibodies against two members of the dynactin family of motor-associated proteins, p50 and $p150^{Glued}$, which are involved in minus-end-directed transport on microtubules[31]. The presence of increased levels of dynein, dynactin p50 and $p150^{Glued}$ in the AMP-PNP-treated sample indicates that increased binding of these motor and motor-associated proteins to microtubules was achieved. These results strongly support the idea that p53 is transported along microtubules by microtubule-based motor proteins. In addition, p53 co-precipitated with both dynactin p50 and dynein IC from A549 cells treated with ADR (Fig. 6b). To establish further the function of dynein in p53 transport, we transfected A549 cells with dynamitin or a β-galactosidase vector (Fig. 6c), and treated them with ADR to stimulate accumulation of p53 in the nucleus. Dynamitin is a member of the dynactin family of motor-associated proteins and its overexpression results in dissociation of dynein from microtubules[32]. Overexpression of dynamitin (Fig. 6c, red) impaired nuclear accumulation of p53 (Fig. 6c, green) after DNA damage, in contrast to neighbouring non-transfected cells

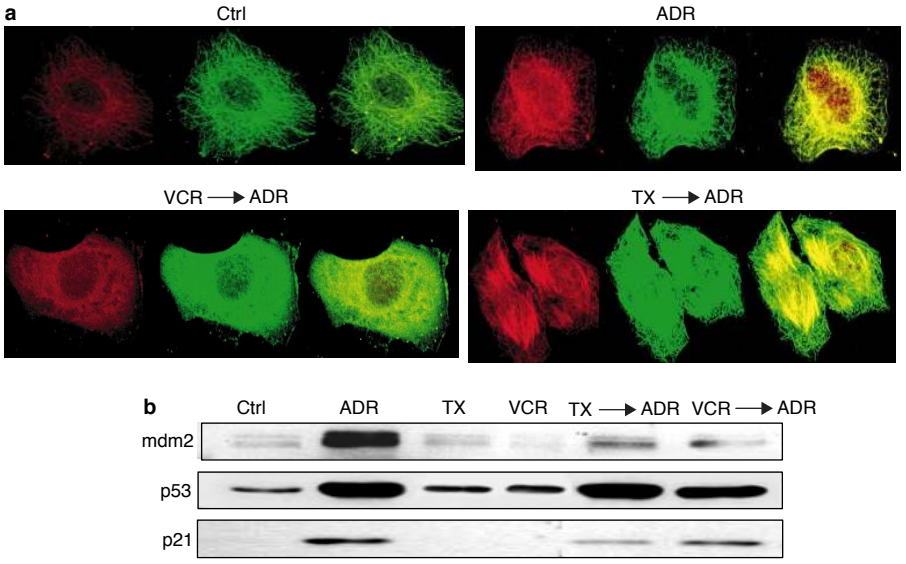

Figure 4 **Microtubule-perturbing drugs impair nuclear accumulation of p53 and induction of mdm2 and p21 after DNA damage.** Cells were plated in duplicate, subjected to the indicated treatments and then processed either for confocal microscopy (**a**) or for western blotting (**b**). **a**, Accumulation of p53 in the nucleus is reduced by microtubule-disrupting drugs. A549 cells were fixed and processed for double immunofluorescence labelling and confocal microscopy as described in Fig. 3, after treatment with adriamycin (ADR) with or without pretreatment with 1 μM vincristine (VCR) or paclitaxel (TX) for 4 h, or after no treatment (Ctrl). p53 is shown in red, α-tubulin in green and co-localization of the two proteins is shown in yellow. Note the inhibition of p53 nuclear accumulation by the VCR ADR and TX ADR treatments, compared with ADR treatment alone. **b**, Treatment with microtubule-disrupting agents before DNA damage impairs the ability of p53 to transactivate Mdm2 and p21. A549 cells were treated for 4 h with 400 ng ml^{-1} ADR either alone or after a 4-h treatment with 1 μM paclitaxel (TX → ADR) or vincristine (VCR → ADR). Untreated A549 cells (Ctrl) and cells treated with 1 μM paclitaxel (TX) or vincristine (VCR) were included as controls. Fifty μg of soluble cell protein from each treatment were immunoblotted with antibodies against p53, mdm2 and p21. Treatment with ADR resulted in induction of mdm2, p53 and p21. However, ADR treatment after treatment with TX or VCR failed to induce mdm2 or p21 compared with ADR alone, whereas p53 induction was unimpaired.

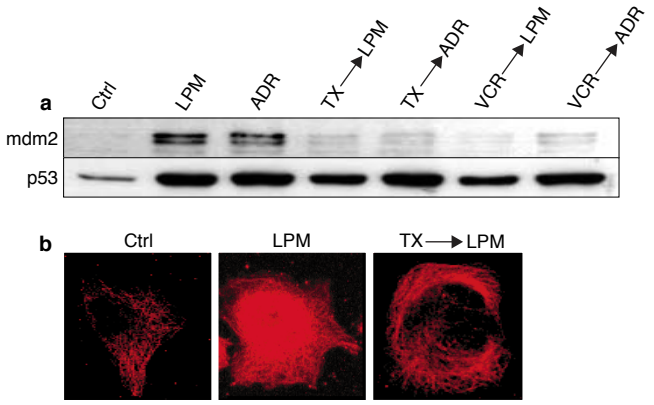

Figure 5 **Pretreatment with paclitaxel or vincristine abrogates the effect of Leptomycin B on p53.** A549 cells were treated with 10 ng ml^{-1} Leptomycin B (LPM) for 5 h, either alone or after treatment with 1 μM paclitaxel (TX → LPM) or vincristine (VCR → LPM) for 2 h. Untreated cells (Ctrl) and cells treated with adriamycin (ADR) instead of LPM were used as controls. **a**, 50 μg of soluble cell protein from each sample were immunoblotted with antibodies against mdm2 and p53 (Ab6). As was the case with ADR, treatment with LPM resulted in increased levels of p53 and mdm2. Pretreatment with TX or VCR before treatment with LPM prevented the induction of mdm2. This result is similar to the TX → ADR and VCR → ADR results, which are shown as controls. **b**, A549 cells treated with 10 ng ml^{-1} LPM for 5 h, either alone or after treatment with 1 μM paclitaxel for 4 h (TX → LPM) were fixed and stained for p53 (red). Treatment with LPM increased levels and nuclear translocation of p53. Pretreatment with paclitaxel inhibited the accumulation of p53 in the nucleus, which is consistent with the lack of mdm2 transactivation seen in **a**.

(Fig. 6c, dashed arrow), in which p53 accumulated in the nucleus after treatment with ADR. The insert in Fig. 6c shows a dynamitin-transfected cell (red) with a predominantly cytoplasmic distribution of p53 (green) after DNA damage. To exclude the possibility that this result was an artefact of the transfection, we transfected cells with a vector encoding β-galactosidase. Accumulation of p53 in the nucleus (Fig. 6c, green) after DNA damage was unimpaired in β-galactosidase-transfected cells (Fig. 6c, red). We microinjected A549 cells with an antibody against the dynein intermediate chain (70.1) before treatment with ADR. In Fig. 6d, a microinjected cell is shown in green (right panel) and p53 is shown in red (left panel). As was the case with overexpression of dynamitin, lack of nuclear accumulation of p53 after DNA damage was observed in the microinjected cell, in contrast to the intense accumulation of p53 in the nucleus that was seen in neighbouring non-injected cells. These results directly implicate the dynein motor protein in transport of p53 to the nucleus.

Purified p53 binds to purified microtubules *in vitro*. We carried out an *in vitro* tubulin-polymerization experiment using RBMT protein or purified rat-brain tubulin (RBT) and purified p53 protein (Pp53; Fig. 7). We combined Pp53 with RBT or RBMT and subjected it to a polymerization cycle in the presence of paclitaxel. After centrifugation, we immunoblotted samples with antibodies against p53, dynein and tubulin. As shown in Fig. 7, p53 associated with microtubules *in vitro*, especially in the presence of tubulin-associated proteins present in RBMT samples, in which case p53 segregated almost exclusively with the polymerized tubulin fraction. RBMT protein, the starting material from which tubulin is purified, also contains structural microtubule-associated proteins (MAPs), such as Map2, Map4, tau and motor proteins (dyneins and kinesins). Immunostaining of dynein (Fig. 7, lower panel) shows that dynein was associated with microtubules (Fig. 7, P) in the

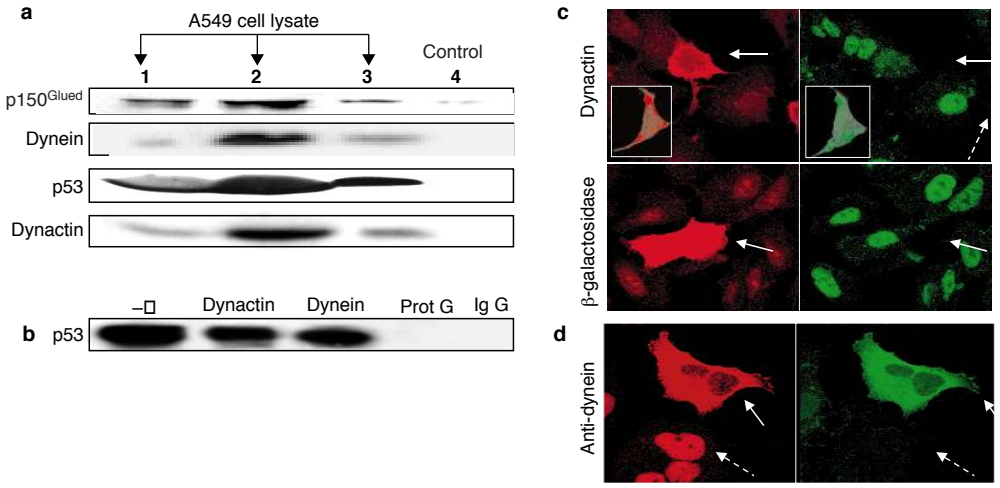

Figure 6 **The microtubule–motor complex dynein/dynactin is involved in transport of p53. a**, The non-hydrolysable ATP analogue AMP-PNP enhances the association of p53 and motor proteins with microtubules. Extracts from adriamycin-treated (400 ng ml^{-1} for 4 h) A549 cells were incubated with (lanes 1 and 2) or without (lane 3) purified microtubules, paclitaxel and GTP at 37 °C for 30 min, allowing polymerization to occur, in the absence (lane 1) or presence (lane 2) of 0.5 mM AMP-PNP. Lane 1, cell extracts supplemented with purified microtubules; lane 2, cell extracts supplemented with purified microtubules in the presence of AMP-PNP; lane 3, cell extracts with AMP-PNP in the absence of microtubules; lane 4, negative control containing exogenous microtubule protein. After centrifugation, pelleted microtubules were analysed by immunoblotting with an anti-p53 (Ab6) antibody or with antibodies against dynein intermediate chain (IC 74) or the motor-associated proteins p50 dynactin and p150^{Glued}. Increased levels of microtubule-associated p53, dynein and motor-associated proteins are present in the sample that received AMP-PNP (lane 2). **b**, p53 co-immunoprecipitates with p50 dynactin and cytoplasmic dynein. 1 mg of soluble cell protein from A549 cells treated with 400 ng ml^{-1} adriamycin for 4 h was immunoprecipitated with an anti-dynactin or with an anti-dynein antibody (IC 74) as indicated, and immunoblotted with an anti-p53 (Ab7) antibody. The lane marked with a minus sign was loaded with 50 μg of soluble cell protein that had not been subjected to immunoprecipitation. Prot G, negative control, containing 1 mg of soluble cell protein immunoprecipitated only with protein G–agarose beads, in the absence of antibody; Ig G, the antibody used for immunoprecipitation, loaded alone.
c, Overexpression of dynamitin impairs the nuclear accumulation of p53 after DNA damage. A549 cells were transiently transfected either with Myc-tagged dynamitin (upper panels) or with β-galactosidase (lower panels). Transfected cells were identified by labelling with anti-c-Myc antibody (red, labelled with rhodamine) or anti-β-galactosidase antibody (red, labelled with rhodamine). Twenty-four hours after transfection, cells were treated with 400 ng ml^{-1} adriamycin for 4 h and p53 was labelled with anti-p53 antibody (green, labelled with FITC). Solid arrows in upper panels show dynamitin-transfected cells; dashed arrow shows a neighbouring non-transfected cell. Inserts show single dynamitin-transfected cells. Solid arrows in lower panels show β-galactosidase-transfected cells with intense nuclear accumulation of p53. **d**, Microinjection with anti-dynein antibody abrogates accumulation of p53 in the nucleus after DNA damage. A549 cells were microinjected with the mouse monoclonal anti-dynein intermediate-chain antibody (70.1) and treated with 400 ng ml^{-1} adriamycin for 4 h. Cells were then fixed and processed for immunofluorescence with antibodies against p53 (Ab7; red, labelled with Texas red); microinjected cells were visualized with a green, FITC-labelled anti-mouse antibody. Right panel shows a microinjected cell (solid arrow); the same cell is shown in the left panel (p53 staining). Note the lack of nuclear accumulation of p53 in the microinjected cell, in contrast to neighbouring non-injected cells (dashed arrows), in which p53 accumulates in the nucleus.

RBMT protein sample. The presence of tubulin-associated proteins in the reaction also enhanced the polymerization of tubulin, as shown by the tubulin immunostaining.

The amino-terminal region of p53 mediates binding to microtubules. We used deletion mutants of p53 to identify the microtubule-binding domain. We used a truncated p53 plasmid lacking the carboxy-terminal 51 amino acids (p53(Δ342–end)). We also created N-terminally truncated p53 constructs lacking between 25 and 100 amino acids from the beginning of the sequence (p53(Δ1–25), p53(Δ1–50), p53(Δ1–75) and p53(Δ1–100)). We assessed the abilities of these p53-deletion mutants to bind to tubulin by co-immunoprecipitation experiments (Fig. 8a) and confocal microscopy (Fig. 8b), after transfection of p53-null PC3 cells with each mutant. Tubulin co-precipitated with p53 from cells transfected with full-length wild-type p53 (Fig. 8a). In contrast, in cells transfected with p53(Δ1–25), p53 did not co-precipitate with tubulin (Fig. 8a). As was the case for full-length p53, p53(Δ342–end) co-precipitated with tubulin (Fig. 8a). PC3 cells transfected with full-length p53 exhibited co-localization of p53 (Fig. 8b, red) with tubulin (Fig. 8b, green) as shown by the presence of yellow colouration in the overlay (Fig. 8b, right). Moreover, p53 staining (Fig. 8b, red) exhibited an intricate and fine microtubule pattern. In cells transfected with p53(Δ1–25) (Fig. 8b), p53 failed to co-localize with microtubules, as shown by the absence of yellow colouration in the overlay, in which two distinct staining patterns exist, the red p53 pattern and the green microtubule pattern. In addition, microtubule structures that were apparent in the tubulin staining pattern were absent from the p53 staining (Fig. 8b, arrows). The other N-terminal p53 deletion mutants (p53(Δ1–50), p53(Δ1–75) and p53(Δ1–100)) all exhibited similar staining patterns to those of p53(Δ1–25) (data not shown). The C-terminal p53 deletion mutant (p53(Δ342–end)) was co-localized with tubulin, as shown by the presence of extensive yellow colouration in the overlay (Fig. 8b) and the microtubule-like staining pattern seen with p53 staining alone (red). These results indicate that the first 25 amino acids of p53 are important for binding of the protein to microtubules.

Discussion

Abnormal cellular localization of p53 has been considered as one of the mechanisms by which p53 can be inactivated. Indeed, the cytoplasmic accumulation of p53 observed in certain human tumours is associated with a defect in p53 function in response to genotoxic stress[17]. However, the mechanisms that regulate the subcellular localization and turnover of p53 are still not well defined.

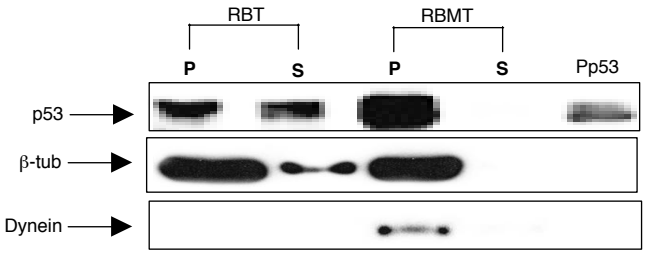

Figure 7, **Purified p53 binds to purified microtubules *in vitro*.** Purified p53 (Pp53) was incubated with purified rat-brain tubulin (RBT) or rat-brain microtubule (RBMT) protein, and subjected to a cycle of polymerization with paclitaxel at 37 °C. After centrifugation, the pellet (P) and supernatant (S) fractions from each reaction were loaded into adjacent wells on SDS–polyacrylamide gels, transferred to Immobilon membrane and immunostained for p53 (Ab2), dynein intermediate chain (IC74), and β-tubulin. Lanes labelled P were loaded with the polymerized form of tubulin (microtubules); lanes labelled S were loaded with soluble tubulin. p53 binds to microtubules, and this binding is enhanced by the presence of tubulin-associated proteins in the RBMT reaction. As shown in by the RBMT pellet sample, RBMT contains dynein that is exclusively associated with microtubules. Pp53, control, containing purified p53 protein loaded alone.

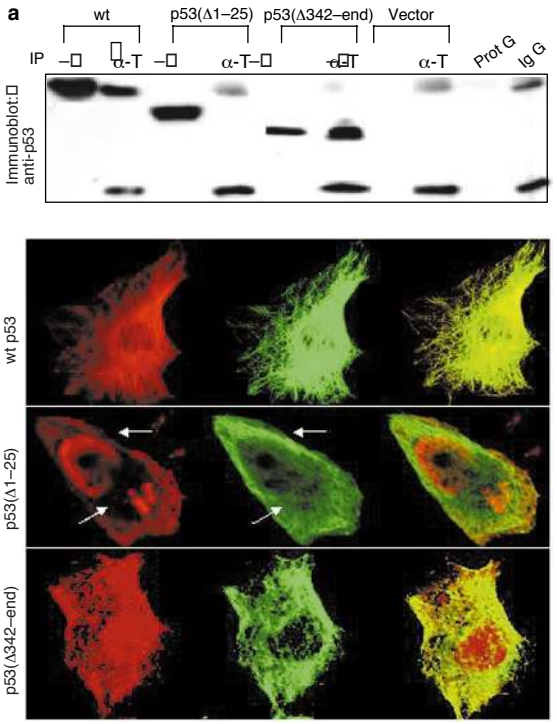

Figure 8 **The N terminus of p53 is important for microtubule binding.** PC3 cells (p53-null) were transiently transfected either with full-length wild-type p53 or with the p53-deletion mutants p53(Δ1–25) and (p53(Δ342–end)). Twenty-four hours after transfection, cells were processed for co-immunoprecipitation and western blotting (**a**) or double immunofluorescence labelling and confocal microscopy (**b**). **a**, p53(Δ1–25) fails to co-precipitate with α-tubulin. Fifty μg of cell protein without immunoprecipitation (–) or 1 mg of cell protein immunoprecipitated (IP) with anti-α-tubulin antibody (α-T) from each transfection (wild-type (wt), p53(Δ1–25), p53(Δ342–end) and vector control), were resolved by SDS–PAGE and immuno stained with a monoclonal anti-p53 antibody (Ab2, directed against amino acids 46–52 of wild-type p53). Note the gradual reduction in size from wild-type p53 to p53(Δ1–25) to p53(Δ342–end) in non-immunoprecipitated samples; this is due to the lower molecular masses of the deletion mutants. p53 is present in immunoprecipitates from wild-type p53 and p53(Δ342–end) transfections; in contrast, p53(Δ1–25) fails to immunoprecipitate with tubulin. Prot G, control, containing cell protein from cells transfected with wild-type p53, incubated with protein-G beads in the absence of antibody; Ig G,control for the heavy chains, containing anti-α-tubulin antibody loaded alone. **b**, p53(Δ1–25) does not co-localize with microtubules in PC3 cells. PC3 cells were transfected with full-length wild-type p53, p53(Δ1–25) or p53(Δ342–end) as indicated. p53 is labelled with anti-p53 (Ab7) antibody (red, labelled with rhodamine) or anti-α-tubulin antibody (green, labelled with FITC). Arrows show distinct microtubules in the α-tubulin staining pattern alone, and the lack of these structures in the p53(Δ1–25) staining pattern.

p53 has been shown to bind to cytoplasmic proteins such as hsc70, hsc84 and F-actin, and to vimentin[33]. However, the biological relevance of the formation of these complexes remains to be determined[34]. A possible interaction between p53 and tubulin has been proposed to occur in the presence of SV40 large T-antigen[35], which is known to stabilize, inactivate and cause overexpression of p53.

We have shown that p53 is normally associated with cellular microtubules and has a preference for polymerized tubulin over soluble α/β-tubulin dimers. Preliminary results from normal human keratinocytes indicate that p53 may also be associated with cellular microtubules in normal cells (data not shown). The association of p53 with cellular microtubules may be important in several ways. First, it may provide a mechanistic basis for regulation of the subcellular localization of p53. Second, our findings indicate that p53 may be an indirect target for microtubule-interacting agents. In this regard, the observation that microtubule-interacting drugs may affect p53 levels[36] and activate p53-dependent checkpoints[4] could be explained by our findings. Third, by binding to microtubules, p53 is brought into close proximity to other cellular proteins. For example, PI3 kinase, which has been shown to bind to microtubules[37], has been implicated in p53 phosphorylation[38]; and BRCA1, which binds to p53 and regulates its expression[39,40], has recently been shown to associate with centrosomes in mitosis and to bind to γ-tubulin, a protein that is essential for microtubule nucleation[41]. Modifications of p53, such as phosphorylation and acetylation, may occur on microtubules. Moreover, p53 may be stored in the cytoplasm bound to microtubules, which may act as a reservoir for p53. This hypothesis is consistent with the substantial amount of p53 that is bound to microtubules and the large capacity of microtubules for storage of p53. This is shown by the ability of microtubules to bind to the higher levels of mutant p53 in 1A9/PTX22 cells, as well as the increased levels of wild-type p53, after damage to DNA (Fig. 3).

Most importantly, our data indicate that the p53–microtubule association is important for accumulation of p53 in the nucleus, as shown by the reduction in accumulation seen after disruption of microtubules with either depolymerizing or polymerizing agents. We have also shown that p53 associates with the microtubule-based motor protein dynein, indicating that p53 may use dynein to translocate from the cytoplasm to the nucleus. As p53 exerts many of its effects by transcriptional regulation, its translocation from cytoplasmic sites of synthesis to nuclear targets is critical for biological responses. Our data showing that disruption of a functional microtubule network before DNA is damaged results in impaired transactivation of p53-targeted genes further supports the idea that microtubules function in intracellular transport of p53. The N terminus of p53 seems to mediate its binding to microtubules; thus, removal of the first 25 amino acids of p53 abolishes its association with microtubules. Future experiments with inducible p53(Δ1–25) will allow a more detailed investigation of the biological significance of the association of p53 with cellular microtubules. □

Methods

Cell lines and antibodies.

Human renal cancer A498 cells, human lung cancer A549 cells and human prostate cancer PC3 cells were obtained from the NCI Drug Screen. A2780 (1A9) human ovarian carcinoma cells and their paclitaxel-resistant subline 1A9/PTX22 were as described[23]. The following monoclonal anti-p53 antibodies were used: anti-p53 (Ab2; monoclonal 1801), anti-p53 (Ab6; monoclonal Do1), anti-p53 (Ab5; monoclonal 1620) and the sheep polyclonal anti-p53 (Ab7). All anti-p53 antibodies were from Oncogene Science (Cambridge, Massachusetts). Anti-α-tubulin (DM1α) and anti-β-tubulin (Tub 2.1) antibodies were from Sigma. Anti-dynactin p50 and anti-p150^{Glued} antibodies were from Transduction Laboratories; anti-p21 and anti-mdm2 antibodies were from Santa Cruz and Calbiochem, respectively. The monoclonal antibody against the intermediate chain of cytoplasmic dynein (IC74) was from Babco (Richmond, California); the monoclonal antibody against dynein intermediate chain (70.1) was from Sigma. Rabbit polyclonal anti-c-Myc antibody was from Santa Cruz; anti-β-galactosidase rabbit polyclonal antibody was from Cortex Biochem (San Leandro, California); mouse monoclonal anti-vimentin antibody was from Sigma. Paclitaxel was from Bristol–Myers Squibb, vincristine was from Eli-Lilly (Indianapolis, Indiana), and colchicine, nocodazole and adriamycin were from Sigma.

Immunoprecipitation and western blotting.

For immunoprecipitation experiments, 1 mg of soluble cell protein was immunoprecipitated with the indicated antibodies, using protein G–agarose (Oncogene Science) as recommended by the manufacturer. Precipitated proteins were resolved by 7.5% SDS–PAGE and immunoblotted with the indicated antibodies. For immunoblotting, 50 μg of soluble cell protein were resolved by SDS–PAGE and immunoblotted with the indicated antibodies.

Temperature-dependent polymerization and depolymerization of microtubules.

Cell pellets from 6×10^8 1A9 or 1A9/PTX22 cells were prepared and frozen from exponentially growing cultures. These were later thawed, resuspended in half-strength MME buffer (0.1 M Mes, 1 mM $MgCl_2$ and 1 mM EGTA, pH 6.9), sonicated twice for 30 s at 0 °C and centrifuged at 30,000 r.p.m. (Ti70 rotor) for 30 min at 4 °C. The supernatant was removed and microtubule protein, prepared as described[42], was added to a final concentration of 1 mg ml^{-1}. GTP was added to a concentration of 1 mM, and then 1 M Mes buffer was added to a final concentration of 0.1 M; the mixture was then incubated at 37 °C for 30 min. Centrifugation (30,000 r.p.m. (Ti70 rotor) for 30 min at 33 °C) yielded the warm pellet (WP) and warm supernatant (WS). The warm pellet was resuspended in MME, kept on ice for 15 min with intermittent sonication to depolymerize the microtubule, and centrifuged (30,000 r.p.m. (Ti70 rotor) for 30 min at 33 °C). This yielded a cold pellet (CP) and a cold supernatant (CS).

Immunofluorescence and microscopy.

Exponentially growing cells were plated on 12-mm glass coverslips (A. Daigger & Co.) and incubated overnight. The following day, after drug treatment, cells were rinsed in PBS and fixed with 3% paraformaldehyde/PBS for 30 min at room temperature. Cells were then fixed in 100% methanol for 5 min at –20 °C and coverslips were rinsed 3 times with PBS and incubated in blocking solution (5% goat serum/PBS) for 1 h at room temperature to reduce non-specific binding of the antibody. All subsequent steps were carried out at room temperature and coverslips were rinsed 3 times in 5% goat serum/PBS between each of the steps. For double-labelling experiments, primary and secondary antibodies were added sequentially for 1 h each. The antibodies used were mouse monoclonal anti-α-tubulin (DM1α) antibody for tubulin/microtubule staining, and sheep polyclonal (Ab7) antibody for p53 staining. A FITC-conjugated anti-mouse antibody, a Texas RedX anti-sheep antibody antibody (both from Vector Laboratories, Lincolnshire, Illinois) and a Rhodamine-RedX anti-rabbit antibody (Jackson Immunochemicals, West Grove, Pennsylvania) were used as secondary antibodies. DNA was counterstained with 1 μg ml^{-1} 4,6-diamidino-2-phenylindole (DAPI, Sigma) in PBS; coverslips were then inverted into 7 μl mounting medium containing antifade agents (Biomeda Corp., Foster City, California) and left at room temperature overnight. Coverslips were examined with a Zeiss axioplasm microscope using a Zeiss ×100 1.3 oil-immersion objective. Confocal images were obtained using an LSM 510 laser-scanning microscope (Zeiss axioplasm).

Purification of p53 and *in vitro* p53–tubulin co-polymerization assay.

Histidine-tagged p53 (His–p53) was expressed and purified essentially as described[43]. Briefly, His–p53 fusion protein was purified from baculovirus-infected Sf9 cells by sonication in lysis buffer (50 mM Tris pH 9.0, 150 mM NaCl, 1 mM β-mercaptoethanol, 0.5% Nonidet P-40, 10% glycerol and COMPLETE protease-inhibitor cocktail (Boehringer)). Soluble protein was purified by nickel-affinity chromatography and was judged to be ~80% pure by SDS–PAGE and silver staining. Purified His–p53 was stored at –80 °C in 25 mM Tris pH 7.0, 150 mM NaCl, 2 mM dithiothreitol and 50% glycerol. Tubulin was purified from RBMT protein[42] by differential polymerization as described[44]. Co-polymerization experiments were carried out in 0.1 M Mes, 1 mM EGTA and 1 mM $MgCl_2$, pH 6.9. Tubulin (20 μM) was pre-assembled in this buffer by addition of 20 μM paclitaxel and 100 μM GTP. After incubation at 37 °C for 20 min, an equal volume of prewarmed recombinant His–p53 was added to a final p53 concentration of ~0.5 μM. After further incubation at 37 °C for 20 min, samples were centrifuged at 100,000*g*. Supernatants and pellets were then collected and prepared for western blotting.

Microtubule co-sedimentation assay.

Microtubule co-sedimentation was assayed as described[45].

Plasmid construction and mutagenesis.

Full-length and truncated p53 were amplified by polymerase chain reaction (PCR) using a pcDNA3.1 vector containing full-length, wild-type p53 as a template. p53 deletion mutants were generated by a PCR SOEing technique[46]. For each p53-deletion mutant, one PCR reaction was carried out using primers designed to define the boundaries of the PCR product. The primers were also designed to introduce *Bam*HI and *Eco*RI sites. The final PCR product with the desired truncation was digested with *Bam*HI and *Eco*RI and purified before ligation into the pcDNA3.1 vector (Invitrogen). p53(Δ342–end) was a gift from C. Harris (NCI, Bethesda, Maryland). The c-Myc-tagged pCMVH50m plasmid containing dynamitin was a gift from R. Vallee (Univ. Massachusets Medical School, Worchester, Massachusetts). The pCMVβ vector expressing β-galactosidase was from Clontech.

Transfection and microinjection assays.

PC3 cells were transiently transfected with full-length p53 or p53 deletion constructs, and A549 cells were transfected with dynamitin or β-gal vector, using the Lipofectamine Plus Reagent (Life Technologies, Inc.) according to the manufacturer's instructions. Twenty-four hours after transfection, PC3 cells were processed for co-immunoprecipitation experiments or double immunofluorescence labelling and confocal microscopy; A549 cells were treated with adriamycin (400 ng ml^{-1} for 4 h) and then processed for double immunofluorescence labelling and confocal microscopy. For the microinjection experiment, A549 cells were microinjected with an antibody against the cytoplasmic dynein intermediate chain (70.1). The antibody was diluted in PBS to a final concentration of 0.1 mg ml^{-1}. Approximately 70 cells were microinjected, and 1 h later they were treated with 400 ng ml^{-1} adriamycin for 4 h. Cells were then fixed and processed for double immunofluorescence labelling and confocal microscopy.

RECEIVED 10 MARCH 2000; REVISED 7 JULY 2000; ACCEPTED 19 JULY 2000;
PUBLISHED 12 SEPTEMBER 2000.

1. Ko, L. J. & Prives, C. p53: puzzle and paradigm. *Genes Dev.* **10,** 1054–1072 (1996).
2. Levine, A. J. p53, the cellular gatekeeper for growth and division. *Cell* **88,** 323–331 (1997).
3. Vogelstein, B. & Kinzler, K. W. p53 function and dysfunction. *Cell* **70,** 523–536 (1992).
4. Cross, S. M. *et al.* A p53-dependent mouse spindle checkpoint. *Science* **267,** 1353–1356 (1995).
5. Fukasawa, K., Choi, T., Kuriyama, R., Rulong, S. & Vande, W. G. Abnormal centrosome amplification in the absence of p53. *Science* **271,** 1744–1747 (1996).
6. Kastan, M. B., Onyekwere, O., Sidransky, D., Vogelstein, B. & Craig, R. W. Participation of p53 protein in the cellular response to DNA damage. *Cancer Res.* **51,** 6304–6311 (1991).
7. Lane, D. P. Cancer. p53, guardian of the genome. *Nature* **358,** 15–16 (1992).
8. Prives, C. Signaling to p53: breaking the MDM2–p53 circuit. *Cell* **95,** 5–8 (1998).
9. el-Deiry, W. S. *et al.* WAF1, a potential mediator of p53 tumor suppression. *Cell* **75,** 817–825 (1993).
10. Miyashita, T. & Reed, J. C. Tumor suppressor p53 is a direct transcriptional activator of the human bax gene. *Cell* **80,** 293–299 (1995).
11. Polyak, K., Xia, Y., Zweier, J. L., Kinzler, K. W. & Vogelstein, B. A model for p53-induced apoptosis. *Nature* **389,** 300–305 (1997).
12. Hollstein, M., Sidransky, D., Vogelstein, B. & Harris, C. C. p53 mutations in human cancers. *Science* **253,** 49–53 (1991).
13. Levine, A. J., Momand, J. & Finlay, C. A. The p53 tumour suppressor gene. *Nature* **351,** 453–456 (1991).
14. Momand, J., Zambetti, G. P., Olson, D. C., George, D. & Levine, A. J. The *mdm-2* oncogene product forms a complex with the p53 protein and inhibits p53-mediated transactivation. *Cell* **69,** 1237–1245 (1992).
15. Oliner, J. D. *et al.* Oncoprotein MDM2 conceals the activation domain of tumour suppressor p53. *Nature* **362,** 857–860 (1993).
16. Scheffner, M., Werness, B. A., Huibregtse, J. M., Levine, A. J. & Howley, P. M. The E6 oncoprotein encoded by human papillomavirus types 16 and 18 promotes the degradation of p53. *Cell* **63,** 1129–1136 (1990).
17. Moll, U. M. *et al.* Cytoplasmic sequestration of wild-type p53 protein impairs the G1 checkpoint after DNA damage. *Mol. Cell. Biol.* **16,** 1126–1137 (1996).
18. Moll, U. M., Riou, G. & Levine, A. J. Two distinct mechanisms alter p53 in breast cancer: mutation and nuclear exclusion. *Proc. Natl Acad. Sci. USA* **89,** 7262–7266 (1992).
19. Schlamp, C. L., Poulsen, G. L., Nork, T. M. & Nickells, R. W. Nuclear exclusion of wild-type p53 in immortalized human retinoblastoma cells. *J. Natl Cancer Inst.* **89,** 1530–1536 (1997).
20. Bosari, S. *et al.* Cytoplasmic accumulation of p53 protein: an independent prognostic indicator in colorectal adenocarcinomas. *J. Natl Cancer Inst.* **86,** 681–687 (1994).
21. Sun, X. F. *et al.* Prognostic significance of cytoplasmic p53 oncoprotein in colorectal adenocarcinoma. *Lancet* **340,** 1369–1373 (1992).
22. Freedman, D. A. & Levine, A. J. Nuclear export is required for degradation of endogenous p53 by MDM2 and human papillomavirus E6. *Mol. Cell Biol.* **18,** 7288–7293 (1998).
23. Giannakakou, P. *et al.* Paclitaxel-resistant human ovarian cancer cells have mutant beta-tubulins that exhibit impaired paclitaxel-driven polymerization. *J. Biol. Chem.* **272,** 17118–17125 (1997).
24. Giannakakou, P. *et al.* Paclitaxel selects for mutant or pseudo-null p53 in drug resistance associated with tubulin mutations in human cancer. *Oncogene* **19,** 3078–3085 (2000).
25. Hyman, A. A. & Karsenti, E. Morphogenetic properties of microtubules and mitotic spindle assembly. *Cell* **84,** 401–410 (1996).
26. Jordan, M. A. & Wilson, L. Microtubules and actin filaments: dynamic targets for cancer chemotherapy. *Curr. Opin. Cell Biol.* **10,** 123–130 (1998).
27. Gundersen, G. G. & Cook, T. A. Microtubules and signal transduction. *Curr. Opin. Cell Biol.* **11,** 81–94 (1999).
28. Stommel, J. M. *et al.* A leucine-rich nuclear export signal in the p53 tetramerization domain: regulation of subcellular localization and p53 activity by NES masking. *EMBO J.* **18,** 1660–1672 (1999).
29. Goodson, H. V., Valetti, C. & Kreis, T. E. Motors and membrane traffic. *Curr. Opin. Cell Biol.* **9,** 18–28 (1997).
30. Okada, Y. & Hirokawa, N. A processive single-headed motor: kinesin superfamily protein KIF1A. *Science* **283,** 1152–1157 (1999).
31. Hirokawa, N. Kinesin and dynein superfamily proteins and the mechanism of organelle transport. *Science* **279,** 519–526 (1998).
32. Burkhardt, J. K., Echeverri, C. J., Nilsson, T. & Vallee, R. B. Overexpression of the dynamitin (p50) subunit of the dynactin complex disrupts dynein-dependent maintenance of membrane organelle distribution. *J. Cell Biol.* **139,** 469–484 (1997).
33. Klotzke, O., Etzrodt, D., Hohenberg, H., Bohn, W. & Deppert, W. Cytoplasmic retention of mutant tsp53 is dependent on an intermediate filament protein (vimentin) scaffold. *Oncogene* **16,**

3423–3434 (1998).
34. Jimenez, G. S., Khan, S. H., Stommel, J. M. & Wahl, G. M. p53 regulation by post-translational modification and nuclear retention in response to diverse stresses. *Oncogene* **18,** 7656–7665 (1999).
35. Maxwell, S. A. *et al.* Simian virus 40 large T antigen and p53 are microtubule-associated proteins in transformed cells. *Cell Growth Differ.* **2,** 115–127 (1991).
36. Blagosklonny, M. V. *et al.* Taxol induction of p21WAF1 and p53 requires c-raf-1. *Cancer Res.* **55,** 4623–4626 (1995).
37. Kapeller, R., Toker, A., Cantley, L. C. & Carpenter, C. L. Phosphoinositide 3-kinase binds constitutively to alpha/beta-tubulin and binds to gamma-tubulin in response to insulin. *J. Biol. Chem.* **270,** 25985–25991 (1995).
38. Magnelli, L. The old and the new in p53 functional regulation. *Biochem. Mol. Med.* **62,** 3–10 (1997).
39. Chai, Y. L. *et al.* The second BRCT domain of BRCA1 proteins interacts with p53 and stimulates transcription from the p21WAF1/CIP1 promoter. *Oncogene* **18,** 263–268 (1999).
40. Ouchi, T., Monteiro, A. N., August, A., Aaronson, S. A. & Hanafusa, H. BRCA1 regulates p53-dependent gene expression. *Proc. Natl Acad. Sci. USA* **95,** 2302–2306 (1998).
41. Hsu, L. C. & White, R. L. BRCA1 is associated with the centrosome during mitosis. *Proc. Natl Acad. Sci.* USA **95,** 12983–12988 (1998).
42. Sackett, D. L., Knipling, L. & Wolff, J. Isolation of microtubule protein from mammalian brain frozen for extended periods of time. *Protein Expr. Purif.* **2,** 390–393 (1991).
43. Takenaka, I., Morin, F., Seizinger, B. R. & Kley, N. Regulation of the sequence-specific DNA binding function of p53 by protein kinase C and protein phosphatases *J. Biol. Chem.* **270,** 5405–5411 (1995).
44. Wolff, J, Sackett, D. L. & Knipling, L. Cation selective promotion of tubulin polymerization by alkali metal chlorides. *Protein Sci.* **5,** 2020–2028 (1996).
45. Balczon, R., Varden, C. E. & Schroer, T. A. Role for microtubules in centrosome doubling in Chinese hamster ovary cells. *Cell Motil. Cytoskeleton* **42,** 60–72 (1999).
46. Horton, R. M., Cai, Z. L., Ho, S. N. & Pease, L. R. Gene splicing by overlap extension: tailor-made genes using the polymerase chain reaction. *Biotechniques* **8,** 528–531 (1990).

ACKNOWLEDGEMENTS
We thank H. Gray and U. Roongta for help with expression and purification of His–p53 fusion protein. We are grateful to M. Clarke and C. Harris for providing full-length wild-type p53 and p53 (Δ342–end) plasmids, respectively. We also thank R. Vallee for providing the dynamitin plasmid, and L. Neckers for providing Leptomycin B. We are indebted to R. Klausner for insightful discussion.
Correspondence and requests for materials should be addressed to P.G.